Biosensors and Bioelectronics 172 (2021) 112762

Contents lists available at ScienceDirect

Biosensors and Bioelectronics

journal homepage: http://www.elsevier.com/locate/bios

Electrochemical biosensing platform based on complex biantennary *N*-glycan for detecting enzymatic sialylation processes

Israel Alshanski [a], Yonatan Sukhran [a], Evgeniy Mervinetsky [a], Carlo Unverzagt [b,**], Shlomo Yitzchaik [a,***], Mattan Hurevich [a,*]

[a] Institute of Chemistry and Center for Nanoscience and Nanotechnology, The Hebrew University of Jerusalem, Safra Campus, Givat Ram, Jerusalem, 91904, Israel
[b] University of Bayreuth, Bioorganic Chemistry, Universitätsstraße 30, 95447, Bayreuth, Germany

ARTICLE INFO

Keywords:
Enzymatic activity detection
Sialylation
Electrochemical impedance spectroscopy
Glycan-protein recognition
Glycan based biosensor

ABSTRACT

Sialylated glycans and glycoproteins are involved in cellular communication and are crucial for distinguishing between signal pathways. Sialylation levels and patterns modulate recognition events and are regulated by the enzymatic activity of sialyltransferases and neuraminidases. Abnormal activity of these enzymes is related to diseases such as cancer and viral infection. Monitoring these enzymatic activities offers valuable diagnostic tools. This work presents an impedimetric biosensing platform for following and detecting sialylation and desialylation processes. This platform is based on a native biantennary *N*-glycan substrate attached to a glassy carbon electrode. Changes in the molecular layer, as a result of enzymatic reactions, were detected by electrochemical impedance spectroscopy, displaying high sensitivity to the enzymatic surface reactions. Increase in the molecular layer roughness in response to the sialylation was visualized using atomic force microscopy. After enzymatic sialylation, the presence of sialic acid was confirmed using cyclic voltammetry by coupling of the redox active marker aminoferrocene. The sialylation showed selectivity toward the *N*-glycan compared to another glycan substrate. A time dependent sialylation was followed by electrochemical impedance spectroscopy, proving that the new system can be applied to evaluate the enzymatic kinetics. Our findings suggest that analyzing sialylation processes using this platform can become a useful tool for the detection of pathological states and pathogen invasion.

1. Introduction

Sialic acid is a monosaccharide with nine backbone carbons. It decorates glycans which are either attached to the cell membrane or secreted to the extracellular matrix. Sialic acid is a common modification of *N*- and *O*- glycoproteins(Schauer and Kamerling, 1997; Traving and Schauer, 1998; Varki, 2007), connected to the glycan via specific linkages and is found mainly at terminal positions(Varki, 2007). The negative charge, unique structure and specific connectivity of sialic acid to the core glycan affect its role in biological events. Sialic acid is involved in many adhesion events, regulates interactions with extracellular proteins, binds and triggers antibodies, and plays a crucial role in the binding of pathogens to glycans on cells(Lewis et al., 2004; Poole et al., 2018; Ströh and Stehle, 2014; Traving and Schauer, 1998; Varki, 2008; Varki and Gagneux, 2012). Overexpression or the lack of sialic acid are related to cancer, inflammation events, HIV and many other diseases(Dennis et al., 1999; Gessner et al., 1993; Kakugawa et al., 2002; Szabo and Skropeta, 2017; Varki, 2008). Bacterial and viral pathogens interact, bind or react with various sialic acid-containing antigens in a specific way(Ströh and Stehle, 2014; Varki, 2008). The recognition patterns of sialylated glycans by cells and pathogens can be very specific and can provide the basis for biosensing platforms for lectins(La Belle et al., 2007), viral infections (Dinh et al., 2014; Hideshima et al., 2013; Hushegyi et al., 2016), and bacterial infections(Xiong et al., 2017).

Recognition of multiantennary sialylated glycans is crucial for the modulation of biological events(Varki, 2007). For example, different strains of influenza viruses recognize sialic acid on target cells via hemagglutinin and enzymatically remove it by a neuraminidase(Von

* Corresponding author.
** Corresponding author.
*** Corresponding author.
E-mail addresses: carlo.unverzagt@uni-bayreuth.de (C. Unverzagt), shlomo.yitzchaik@mail.huji.ac.il (S. Yitzchaik), mattan.hurevich@mail.huji.ac.il (M. Hurevich).

https://doi.org/10.1016/j.bios.2020.112762
Received 27 July 2020; Received in revised form 3 September 2020; Accepted 22 October 2020
Available online 24 October 2020

Itzstein, 2007; Von Itzstein et al., 1993). Different sialyltransferases or neuraminidases can be distinguished based on their reaction kinetics with specific and complex *N*-glycan or *O*-glycan substrates(Von Itzstein, 2007). Following the glycan-dependent enzymatic sialylation and desialylation processes can be useful to detect pathogens(Ströh and Stehle, 2014; Von Itzstein, 2007) or monitor pathologic conditions(Bao et al., 2015; Yang et al., 2015). Selective biosensors that are based on complex sialylated glycans can be used to detect pathogens, monitor tumor growth or immune response and can provide valuable information on disease progress and on treatment efficiency(Belický et al., 2016; Bertok et al., 2013; Li et al., 2019). Although simple di- or trisaccharides can be used as substrates to follow and monitor sialylation events(Lopez Aguilar et al., 2018), they lack the complexity of native multiantennary glycans, which is crucial for tuning the specificity of biological recognition(Fukushima et al., 1984; Takada et al., 1993; Itzkowitz et al., 1990; Yonezawa and Sato, 1997). Well-defined complex sialylated glycans are not readily available. The isolation of multiantennary *N*-glycans results in mixtures, which cannot be used to probe bio-recognition. Bottom-up preparation is the only way to access homogenous *N*-glycans and is currently done by a combination of chemical and chemoenzymatic approaches, requires significant synthetic and analytical efforts and usually provides only limited amounts of pure material (André et al., 2004; Ito et al., 1993; Raman et al., 2005). Since homogeneous *N*-glycans are difficult to make and are available only in small quantities, elucidating their biological roles is not straightforward and calls for the development of novel tools to study and use them(Torii et al., 2014).

Fluorescently or NIR-labelled glycans are frequently used to monitor enzymatic glycan processing and pathogen activity. These techniques require labeling of the glycan synthetically, which can be challenging when only small amounts of complex glycans are available. Furthermore, the output of the enzymatic conversion cannot be translated directly into a measurable electrical signal(Burke et al., 2015; Shieh et al., 2014). On the other hand, electrochemical strategies are extremely sensitive, their selectivity can be easily tailored, they provide a fast response, can translate interaction events directly into a measurable electrical signal and are used as point of care devices(Adamson et al., 2012; Butler et al., 2019; Dechtrirat et al., 2014; Gray et al., 2013; Lisdat and Schäfer, 2008; Tang et al., 2018).

Electrochemical impedance spectroscopy (EIS) is a sensitive and label-free analytical technique that can be used for the detection of biological events including the recognition of pathogens(Adamson et al., 2012; Butler et al., 2019; Lisdat and Schäfer, 2008; Zhang et al., 2017). Since the EIS signal relies on surface modifications, it is highly sensitive to the organization of the monolayer and can be used to detect interactions at low concentrations or follow enzymatic processes. EIS proved useful for monitoring enzymatic phosphorylation and dephosphorylation as well as enzymatic glycosylations and hydrolysis of simple glycans(Chen et al., 2016; Hou et al., 2006; Snir et al., 2011). EIS based on oligonucleotides and peptides is already wide spread but glycan-based biosensing is still in its infancy. We have recently demonstrated that tiny amounts of complex sulfated glycans can be anchored to glassy carbon surfaces via a covalent linkage and used for detecting low concentrations of metal ions(Alshanski et al., 2019). These encouraging results proved that EIS can be a powerful tool to explore the biology of complex glycans and use them as a sensing layer. EIS-based enzymatic hydrolysis of glycans has been performed with small glycans mainly because they are more readily available, hence, the complexity of the natural glycan entities is not fully exploited for sensing. Sialylation leads to the addition of a negatively charged and bulky monosaccharide, thus significantly changing the properties of the layer(Zhao et al., 2008), which can be translated into an impedimetric signal. Label-free EIS detection of enzymatic sialylation and desialylation using a complex-type *N*-glycan may enable differentiation between pathogens and pathological states and can be done using only small quantities of these entities.

This work presents a label-free electrochemical platform for monitoring the sialylation and desialylation of a complex biantennary *N*-glycan (Fig. 1). A glassy carbon electrode (GCE) functionalized with biantennary *N*-glycan was used to measure the impedimetric response of enzymatic sialylation and desialylation. These processes were also followed by cyclic voltammetry (CV) and atomic force microscopy (AFM). Time-dependent impedimetric analysis was used to establish the kinetic parameters of the sialylation process. The reversibility of the process was evaluated by EIS and AFM.

2. Results and discussion

Sensing of sialylation and desialylation processes requires a glycan substrate attached to a modified electrode (Fig. 1). A biantennary *N*-glycan (**A**) with two terminal galactose moieties (**A**) was synthesized and equipped with an azide on the reducing end (Scheme S1).(Ullmann et al., 2012) The azide moiety enables anchoring of the glycan to surfaces via click reaction while the two terminal galactose moieties serve as substrates for sialylation using α-2,6-sialyltransferase (ST)(Alshanski et al., 2019; Sletten and Bertozzi, 2011). In our process, **A** was attached to a dibenzocyclooctyne (DBCO) modified GCE surface via copper-free strain-promoted bio-click reaction to produce the glycosylated electrode **(**GCE-**A)** (Scheme S2).(Alshanski et al., 2019; Sletten and Bertozzi, 2011) The assembly of GCE-**A** was characterized by EIS and the modified electrode was used to study the electrochemical signal produced in response to enzymatic sialylation processes.

In order to study the impedimetric response, sialylation was performed on GCE-**A** using α-2,6-ST from *Photobacterium damsela* in the presence of Cytidine-5′-monophospho-N-acetylneuraminic (CMP-Neu5Ac) (Detailed procedure in SI). The resistance for redox-active $[Fe(CN)_6]^{3-}/[Fe(CN)_6]^{4-}$ couple penetration (charge transfer resistance, R_{CT}) through the monolayer was measured before and after sialylation (see Nyquist plot, Fig. 2a). Sialylation of GCE-**A** to give GCE-**SiaA** resulted in an increase of R_{CT} by a factor of 1.9 (Fig. 2b, red). This increase in resistance can be explained by the additional charge and hindrance as a result of the sialylation leading to changes in the density and electrostatic repulsion from the glycan layer. As a control, the sialylation of GCE-**A** was attempted with ST but without CMP-Neu5Ac resulting only in a negligible change of the measured R_{CT} (Fig. 2b, blue). This suggests that the signal measured after incubation in presence of CMP-Neu5Ac corresponds to enzymatic addition of the sialic acid and not to the adhesion or binding of the enzyme. Sialylation was also performed on a GCE functionalized with maltose (Fig. 2b, green). Maltose is not a natural substrate for ST because it has a terminal glucose moiety instead of a galactose, hence it is not expected to undergo sialylation. Indeed, incubation of GCE-maltose with ST and CMP-Neu5Ac did not result in a significant increase of R_{CT}. The passivity of the maltose surface proved that the change in R_{CT} observed for **A** is a result of a selective enzymatic sialylation of the terminal galactose moieties. The above results demonstrated that the enzymatic sialylation occurred only on the natural substrate and in the presence of all components. Thus, the EIS response was not related to binding or adsorption of the protein but to its activity. This suggests that EIS using GCE-**A** can be used as a platform for analyzing transformations by enzymatic sialylation.

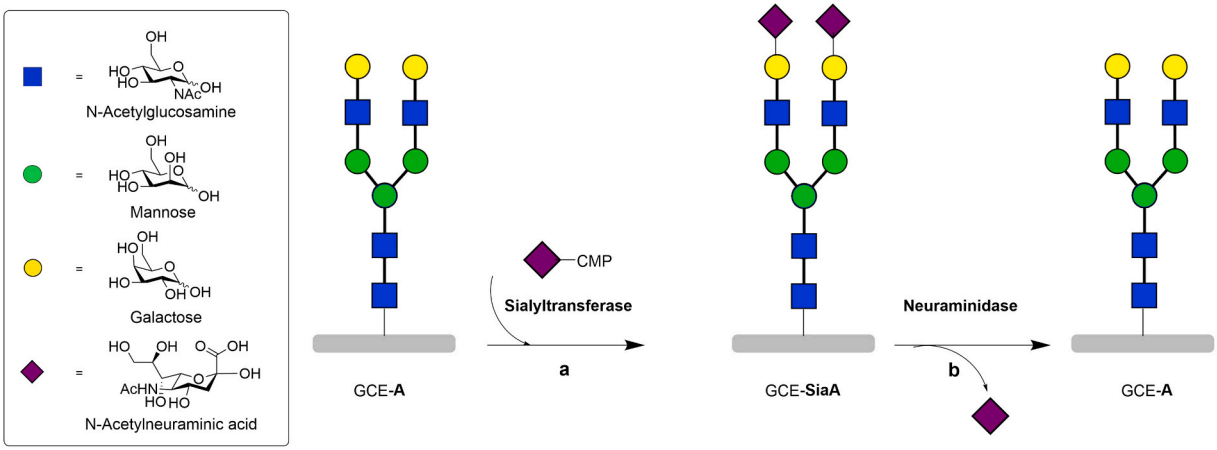

Fig. 1. Enzymatic processes on complex N-glycan (**A**) attached to an electrode (GCE) can be monitored by EIS. a**)** Sialylation of galactose-terminated glycan using CMP-Neu5Ac and sialyltransferase (ST) b**)** Desialylation using neuraminidase removes the sialic acid from the glycan. Both enzymatic reactions result in impedimetric response.

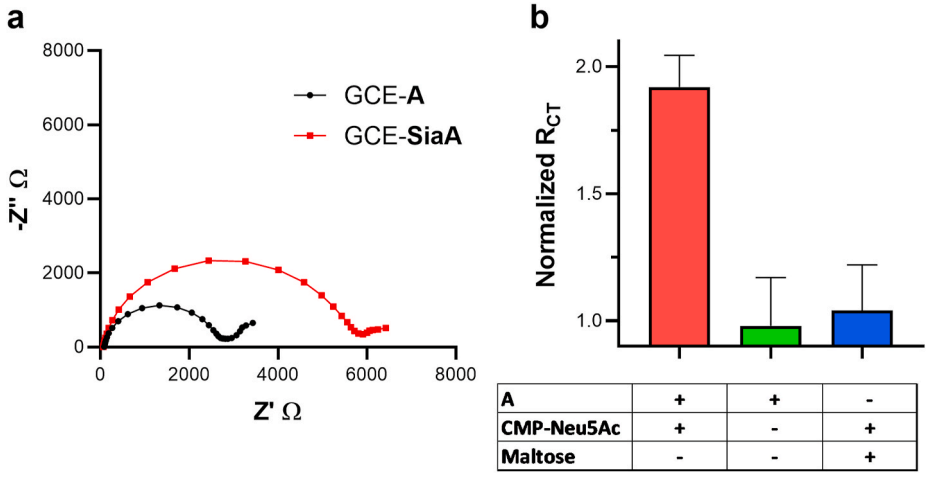

Fig. 2. Impedimetric response of glycan layer to enzymatic sialylation. a) Nyquist plot of GCE-**A** (black) and GCE-**SiaA** (red). b) Normalized R_{CT} after incubation of ST with: GCE-**A** and CMP-Neu5Ac (red). GCE-**A** without CMP-Neu5Ac (green). Maltose-modified-GCE and CMP-Neu5Ac (blue). The error bars are based on standard deviation between three electrodes. (For interpretation of the references to colour in this figure legend, the reader is referred to the Web version of this article.)

Enzymatic reactions on modified surfaces can lead to a time-dependent change in the glycan-layer properties which is an indication for the kinetics of the process (Saum et al., 1998). Following the kinetics of a sialylation can provide valuable information on the type, reactivity and specificity of a ST and may be correlated with immunological events, pathogen infection and more. Time response profile studies of the GCE-**A** sialylation were performed using EIS. The electrodes were exposed to a solution of ST and CMP-Neu5Ac for 5–120 min (see SI). EIS measurements after each exposure showed a time-dependent increase in R_{CT} (Fig. 3). After 120 min of enzymatic sialylation, the R_{CT} increased by 50%

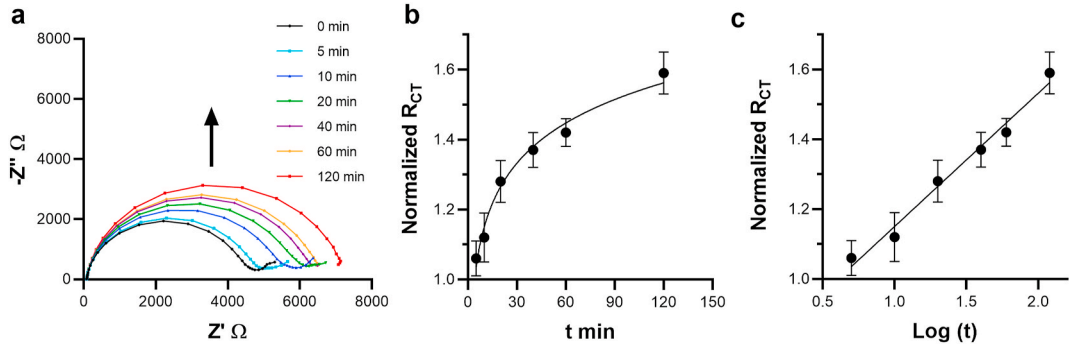

Fig. 3. *Time-dependent EIS response of GCE-**A** to ST. a) Nyquist plot measured after enzymatic reaction for 0 to* 120 min. b) Time-dependent normalized R_{CT}. c) Linear correlation of normalized R_{CT} to log (t) which fits an equation of $NR_{CT} = (0.38 \pm 0.05) \cdot log(t) + (0.77 \pm 0.07)$. Standard deviation is based on four different electrodes. All values are normalized by the R_{CT} value of GCE-**A**.

compared with GCE-**A** (Fig. 3b), while up to 90% increase was measured after 8 h of incubation (Fig. 2b). This correlation between the R_{CT} value and time indicates a gradual change in the dielectric properties of the glycan-layer as a result of the enzymatic transformation which is in line with previous studies(Saum et al., 1998). These changes showed that the exposure to a sialylation solution follows time-dependent kinetics, which fit the following correlation: $NR_{CT} = (0.38 \pm 0.05) \cdot \log(t) + (0.77 \pm 0.07)$. The time-dependent behavior observed above suggests that different STs may be discriminated based on their specific sialylation kinetics profile and not only by a binary type of signal transduction output. Decreasing the enzyme concentration by a factor of 10 also provided a time dependent increase in impedance, albeit with, faster kinetics (Fig. S3). The decrease in the reaction rate, when high concentration of the enzyme is used, impies that there is a steric hinderence around the substarte. This suboptimal response suggests that further optimization of the system is required.

Aminoferrocene was used as a selective marker to confirm and quantify the amount of sialic acid after the enzymatic sialylation of GCE-**A**. Aminoferrocene has very distinctive oxidation and reduction peaks that can be detected and quantified by CV(Gray et al., 2013; Song et al., 2002). Furthermore, it reacts with the carboxyl moiety, which can only be present on GCE-**SiaA** and not on GCE-**A**. Both GCE-**A** and GCE-**SiaA** were treated with aminoferrocene and the CV was measured following the reaction. (Albericio and El-faham, 2018; Mervinetsky et al., 2020; Naoum et al., 2019) (Fig. 4a). The CV of GCE-**SiaA** showed a signal at an oxidation potential of approximately 0.4 V which is typical for ferrocene (Fig. 4b), while this peak was not observed for GCE-**A** (Fig. S4).(Cuartero et al., 2019) Since ferrocene-specific signals appeared for GCE-**SiaA** and not for GCE-**A**, it is a clear indication that sialylation took place, further confirming that R_{CT} increase corresponded to enzymatic sialylation. Additionally, the ferrocene was quantified to give a surface number density of $9.6 \cdot 10^{12}$ molecules$\cdot$cm^{-2} (SI), which correlates to 12% sialylation coverage when comparing to the calculated diameter of SiaA (calculation from Chem3D, see Fig. S6).

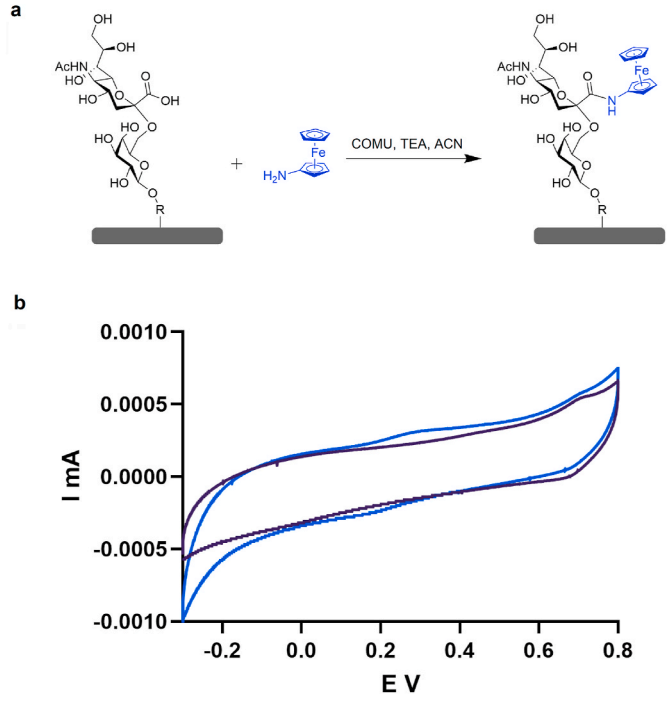

Fig. 4. Cyclic voltammetry of redox active sialylation marker. a) Coupling of aminoferrocene to GCE-**SiaA**. b) CV scan from −0.3 V to 0.8 V with a scan rate of 50 mV/s before (black) and after (blue) reaction of GCE-**SiaA** with 50 mM of aminoferrocene. (For interpretation of the references to colour in this figure legend, the reader is referred to the Web version of this article.)

Desialylation, the hydrolysis of sialic acid, is an enzymatic reaction involved in many pathogenic and cell communication events. To evaluate if EIS can also be used to monitor desialylation, GCE-**SiaA** was incubated with neuraminidase from *Arthrobacter ureafaciens* (Merck) using an established desialylation procedures (S4)(Jung et al., 1989). Desialylation of GCE-**SiaA** resulted in a significant decrease in R_{CT} values (Fig. 5a). The decrease in R_{CT} shows that the surface becomes more similar to the non sialylated GCE-**A**. This indicates that the sialic acid was removed from GCE-**SiaA**. The desialylation did not revert the system to the initial R_{CT} values before sialylation (Fig. 5b). We assume that this might be a result of either incomplete desialylation or of a reorganization of the monolayer. To check the reversibility of the enzymatic processes, a second sialylation was performed after desialylation of GCE-**SiaA**. The R_{CT} after the second sialylation was virtually the same as after the first sialylation (Fig. 5b). This indicates that reversible enzymatic sialylation processes on GCE can be detected by EIS.

Surface topography of glycan-modified silicon wafers were analyzed by AFM to visualize the changes of the layer in response to enzymatic modifications. DBCO-modified silicon wafers were prepared for surface characterizations and analyzed using variable angle spectroscopic ellipsometry, confirming consistence and pinhole free modification (Alshanski et al., 2019). These wafers were acetylated following the coupling of DBCO and a bio-click reaction of **A**. The wafers were analyzed by AFM and contact angle (CA) measurements. The *N*-acetylated DBCO layer had a roughness of 0.12 nm (Fig. S5) and a CA of 72° indicating a hydrophobic outer layer. The surfaces modified with **A** had a roughness of 0.15 nm (Fig. 6a) and a more hydrophilic layer with a CA of 50°. These changes of the monolayer properties support the modification with the *N*-glycan. Sialylation of the glycosylated surface increased the layer roughness to 0.31 nm (Fig. 6b), while the desialylation restored the smoother surface with a roughness of 0.11 nm (Fig. 6c). These results suggest that the enzymatic reactions of the glycan lead to changes in the surface properties. It shows that the roughness increases by the addition of the bulky and negatively charged sialic acid whereas the surface smoothens when this moiety is removed. The AFM analysis correlates with the EIS response where the impedance increases with the addition of sialic acid while decreases when sialic acid is removed. AFM also allowed us to visualize the reversibility of the enzymatic transformations by detecting changes of the surface properties further proving the observations by EIS. A similar phenomenon was observed for enzymatic phosphorylation and dephosphorylation reactions of a peptide monolayer on an Au electrode(Snir et al., 2011; Zhuravel et al., 2016). The native peptide monolayer had a smooth topography that was roughened by the phosphorylation reaction, mainly due to electrostatic repulsion of the negatively charged phosphate groups, and smoothened by the dephosphorylation reaction to the original value of the neutral nanapeptide monolayer.

3. Conclusions

A robust strategy enabled us to anchor the complex biantennary *N*-glycan azide **A** to oxide surfaces and to use the functionalized surface for the development of a biosensing platform capable of monitoring enzymatic sialylation and desialylation processes. To our knowledge, this is the first time that a native complex *N*-glycan was used for electrochemical sensing. We showed that EIS response can be correlated directly with the enzymatic addition or removal of sialic acid from the anchored *N*-glycan. The enzymatic processes were monitored, characterized and analyzed using impedimetric/voltammetric analyses, wettability studies and AFM-based topography imaging. EIS analysis provided us with a tool to evaluate the time-dependent response of the enzymatic processes and was used to follow the sialylation/desialylation cycle. The ability to monitor time-dependent enzymatic sialylation using EIS can lead to the development of a new line of biosensors providing an electrical output that correlates with a process rather than a single event response. We proved that minute amounts of a complex *N*-glycan are

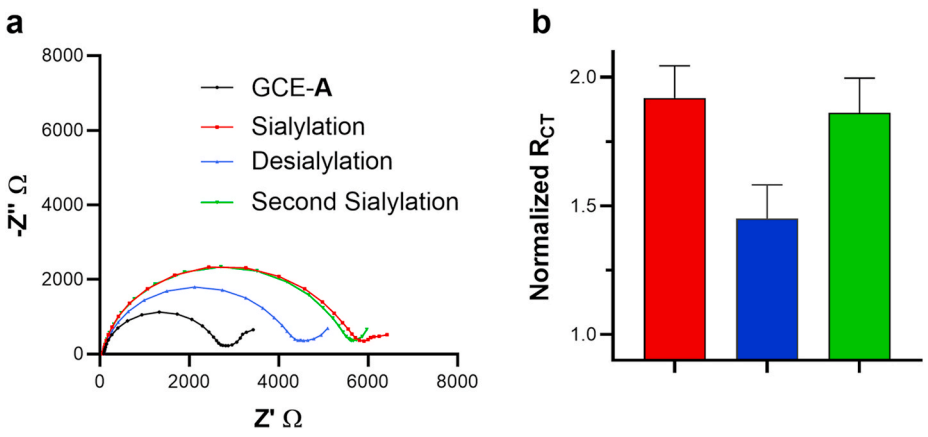

Fig. 5. *Sialylation/desialylation cycles. a) Nyquist plot of the EIS measurements for the sialylation and desialylation cycles b) Normalized impedimetric response of GCE-**A** to a sialylation and desialylation cycle.* ***Red****, response after the first sialylation.* ***Blue****, the response after desialylation.* ***Green****, the response after the second sialylation. The values of the measurements are normalized to the value of the electrode before the first sialylation. The error bars are based on standard deviation between three electrodes.* (For interpretation of the references to colour in this figure legend, the reader is referred to the Web version of this article.)

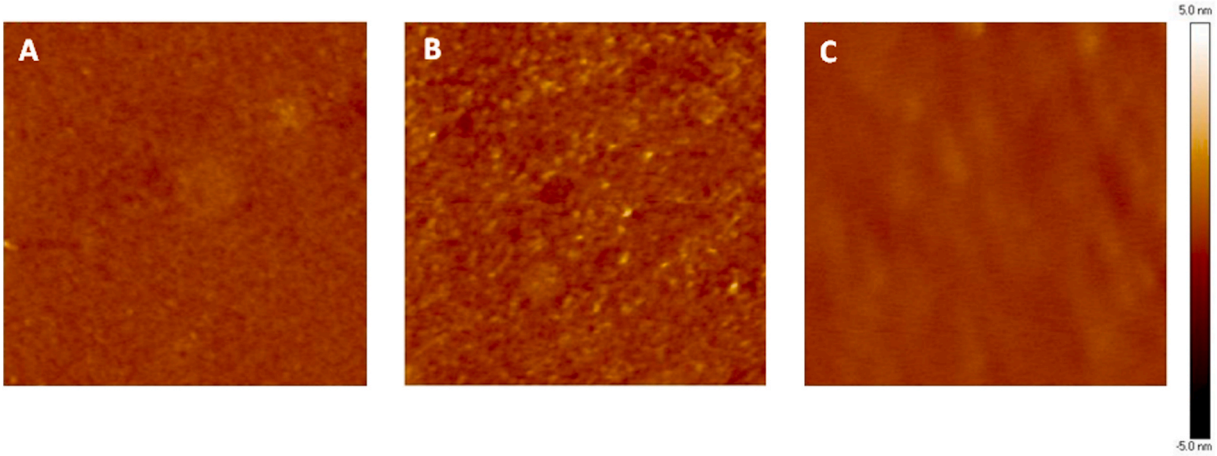

Fig. 6. AFM analyses of N-glycan-modified Si wafers, 1 × 1 μm × μm. a) After attachment of **A** via click chemistry, RMS roughness = 0.15 nm. b) After sialylation, RMS roughness = 0.31 nm. c) After desialylation, RMS roughness = 0.11 nm.

sufficient to generate a sensing platform that enables following reversible enzymatic transformations by EIS. The combination of a surface-immobilized native *N*-glycan and EIS opens a new route for the sensing of processes related to pathogen infection and pathologic conditions, which complements the specific biomarker detection strategy.

CRediT authorship contribution statement

Israel Alshanski: Formal analysis, Data curation, Writing - original draft, Experimented, analyzed the data, and wrote the original manuscript draft preparation. **Yonatan Sukhran:** Formal analysis, Data curation, Experimented, analyzed the data, and edited the paper. **Evgeniy Mervinetsky:** Experimented and characterized the surfaces. **Carlo Unverzagt:** Writing - original draft, Synthesized the glycan, conceived the original idea and planned the experiments, wrote, reviewed, and edited the manuscript. **Shlomo Yitzchaik:** Writing - review & editing, Supervision, Conceived the original idea and planned the experiments. Supervised the project, wrote, reviewed, and edited the paper. **Mattan Hurevich:** Writing - review & editing, Supervision, Conceived the original idea and planned the experiments. Supervised the project, wrote, reviewed, and edited the paper.

Declaration of competing interest

The authors declare that they have no known competing financial interests or personal relationships that could have appeared to influence the work reported in this paper.

Acknowledgments

IA is supported by the Hebrew University Center for Nanoscience and Nanotechnology PhD. Scholarship. SY is the Benjamin H. Birstein chair in chemistry. CU thanks the Deutsche Forschungsgemeinschaft for funding (UN 63/4–2).

Appendix A. Supplementary data

Supplementary data to this article can be found online at https://doi.org/10.1016/j.bios.2020.112762.

References

Adamson, T.L., Eusebio, F.A., Cook, C.B., Labelle, J.T., 2012. Analyst 137, 4179–4187. https://doi.org/10.1039/c2an35645g.
Albericio, F., El-faham, A., 2018. Org. Process Res. Dev. 22, 760–772. https://doi.org/10.1021/acs.oprd.8b00159.
Alshanski, I., Blaszkiewicz, J., Mervinetsky, E., Rademann, J., Yitzchaik, S., Hurevich, M., 2019. Chem. Eur J. 25, 12083–12090. https://doi.org/10.1002/chem.201901538.
André, S., Unverzagt, C., Kojima, S., Frank, M., Seifert, J., Fink, C., Kayser, K., Von Der Lieth, C.W., Gabius, H.J., 2004. Eur. J. Biochem. 271, 118–134. https://doi.org/10.1046/j.1432-1033.2003.03910.x.
Bao, L., Ding, L., Yang, M., Ju, H., 2015. Sci. Rep. 5, 1–11. https://doi.org/10.1038/srep10947.
Belický, Š., Katrlík, J., Tkáč, J., 2016. Essays Biochem. 60, 37–47. https://doi.org/10.1042/EBC20150005.
Bertok, T., Sediva, A., Katrlik, J., Gemeiner, P., Mikula, M., Nosko, M., Tkac, J., 2013. Talanta 108, 11–18. https://doi.org/10.1016/j.talanta.2013.02.052.
Burke, H.M., Gunnlaugsson, T., Scanlan, E.M., 2015. Chem. Commun. 51, 10576–10588. https://doi.org/10.1039/c5cc02793d.

Butler, D., Goel, N., Goodnight, L., Tadigadapa, S., Ebrahimi, A., 2019. Biosens. Bioelectron. 129, 269–276. https://doi.org/10.1016/j.bios.2018.09.057.
Chen, Z., Zhang, L., Liu, Y., Li, J., 2016. J. Electroanal. Chem. 781, 83–89. https://doi.org/10.1016/j.jelechem.2016.05.034.
Cuartero, M., Chai, L., Zhang, B., De Marco, R., Crespo, G.A., 2019. Electrochim. Acta 315, 84–93. https://doi.org/10.1016/j.electacta.2019.05.091.
Dechtrirat, D., Gajovic-Eichelmann, N., Wojcik, F., Hartmann, L., Bier, F.F., Scheller, F. W., 2014. Biosens. Bioelectron. 58, 1–8. https://doi.org/10.1016/j.bios.2014.02.028.
Dennis, J.W., Granovsky, M., Warren, C.E., 1999. Biochim. Biophys. Acta Gen. Subj. 1473, 21–34. https://doi.org/10.1016/S0304-4165(99)00167-1.
Dinh, H., Zhang, X., Sweeney, J., Yang, Y., He, Y., Dhawane, A., Iyer, S.S., 2014. Anal. Chem. 86, 8238–8244. https://doi.org/10.1021/ac501624v.
Fukushima, K., Hirota, M., Wakisaka, A., Togashi, H., Chia, D., Suyama, N., Fukushi, Y., Nudelman, E., Hakomori, S.I., Terasaki, P.I., 1984. Canc. Res. 44, 5279–5285.
Gessner, P., Riedl, S., Quentmaier, A., Kemmner, W, 1993. Canc. Lett. 75, 143–149. https://doi.org/10.1016/0304-3835(93)90056-F.
Gray, C.J., Weissenborn, M.J., Eyers, C.E., Flitsch, S.L., 2013. Chem. Soc. Rev. 42, 6378–6405. https://doi.org/10.1039/c3cs60018a.
Hideshima, S., Hinou, H., Ebihara, D., Sato, R., Kuroiwa, S., Nakanishi, T., Nishimura, S. I., Osaka, T., 2013. Anal. Chem. 85, 5641–5644. https://doi.org/10.1021/ac401085c.
Hou, Y., Helali, S., Zhang, A., Jaffrezic-Renault, N., Martelet, C., Minic, J., Gorojankina, T., Persuy, M.A., Pajot-Augy, E., Salesse, R., Bessueille, F., Samitier, J., Errachid, A., Akimov, V., Reggiani, L., Pennetta, C., Alfinito, E., 2006. Biosens. Bioelectron. 21, 1393–1402. https://doi.org/10.1016/j.bios.2005.06.002.
Hushegyi, A., Pihíková, D., Bertok, T., Adam, V., Kizek, R., Tkac, J., 2016. Biosens. Bioelectron. 79, 644–649. https://doi.org/10.1016/j.bios.2015.12.102.
Ito, Y., Gaudino, J.J., Paulson, J.C., 1993. Pure Appl. Chem. 65, 753–762. https://doi.org/10.1351/pac199365040753.
Itzkowitz, S.H., Bloom, E.J., Kokal, W.A., Modin, G., Hakomori, S.-I., Kim, Y.S., 1990. Sialosyl-Tn. Cancer 60, 1960–1966. https://doi.org/10.1002/1097-0142(19901101)66:9<1960::AID-CNCR2820660919>3.0.CO;2-X.
Jung, K., Pergande, M., Klotzek, S., 1989. Clin. Chem. 35, 1955–1957. https://doi.org/10.1093/clinchem/35.9.1955.
Kakugawa, Y., Wada, T., Yamaguchi, K., Yamanami, H., Ouchi, K., Sato, I., Miyagi, T., 2002. Proc. Natl. Acad. Sci. U.S.A. 99, 10718–10723. https://doi.org/10.1073/pnas.152597199.
La Belle, J.T., Gerlach, J.Q., Svarovsky, S., Joshi, L., 2007. Anal. Chem. 79, 6959–6964. https://doi.org/10.1021/ac070651e.
Lewis, A.L., Nizet, V., Varki, A., 2004. Proc. Natl. Acad. Sci. U.S.A. 101, 11123–11128. https://doi.org/10.1073/pnas.0403010101.
Li, J., He, J., Zhang, C., Chen, J., Mao, W., Yu, C., 2019. Biosens. Bioelectron. 130, 166–173. https://doi.org/10.1016/j.bios.2019.01.054.
Lisdat, F., Schäfer, D., 2008. Anal. Bioanal. Chem. 391, 1555–1567. https://doi.org/10.1007/s00216-008-1970-7.
Lopez Aguilar, A., Meng, L., Hou, X., Li, W., Moremen, W., Wu, P., 2018. Bioconjugate Chem. 29, 1231–1239. https://doi.org/10.1021/acs.bioconjchem.8b00021.
Mervinetsky, E., Alshanski, I., Tadi, K.K., Dianat, A., Buchwald, J., Gutierrez, R., Cuniberti, G., Hurevich, M., Yitzchaik, S., 2020. J. Mater. Chem. B 8, 155–160. https://doi.org/10.1039/c9tb01932d.
Naoum, J., Alshanski, I., Gitlin Domagalska, A., Bentolila, M., Gilon, C., Hurevich, M., 2019. Org. Process Res. Dev. 23, 2733–2739. https://doi.org/10.1021/acs.oprd.9b00398.
Poole, J., Day, C.J., Von Itzstein, M., Paton, J.C., Jennings, M.P., 2018. Nat. Rev. Microbiol. 16, 440–452. https://doi.org/10.1038/s41579-018-0007-2.
Raman, R., Raguram, S., Venkataraman, G., Paulson, J.C., Sasisekharan, R., 2005. Nat. Methods 2, 817–824. https://doi.org/10.1038/nmeth807.
Saum, A.G.E., Cumming, R.H., Rowell, F.J., 1998. Biosens. Bioelectron. 13, 511–518. https://doi.org/10.1016/S0956-5663(97)00129-2.
Schauer, R., Kamerling, J.P., 1997. Glycoproteins II. https://doi.org/10.1016/S0167-7306(08)60624-9, 243-402.
Shieh, P., Siegrist, M.S., Cullen, A.J., Bertozzi, C.R., 2014. Proc. Natl. Acad. Sci. U.S.A. 111, 5456–5461. https://doi.org/10.1073/pnas.1322727111.
Sletten, E.M., Bertozzi, C.R., 2011. Acc. Chem. Res. 44, 666–676. https://doi.org/10.1021/ar200148z.
Snir, E., Joore, J., Timmerman, P., Yitzchaik, S., 2011. Langmuir 27, 11212–11221. https://doi.org/10.1021/la202247m.
Song, H., Kerman, K., Kraatz, H.B., 2002. Chem. Commun. 8, 502–504. https://doi.org/10.1039/b714383d.
Ströh, L.J., Stehle, T., 2014. Annu. Rev. Virol. 1, 285–306. https://doi.org/10.1146/annurev-virology-031413-085417.
Szabo, R., Skropeta, D., 2017. Med. Res. Rev. 37, 219–270. https://doi.org/10.1002/med.21407.
Takada, A., Ohmori, K., Yoneda, T., Tsuyuoka, K., Hasegawa, A., Kiso, M., Kannagi, R., 1993. Canc. Res. 354–361.
Tang, Y.H., Lin, H.C., Lai, C.L., Chen, P.Y., Lai, C.H., 2018. Biosens. Bioelectron. 116, 100–107. https://doi.org/10.1016/j.bios.2018.05.002.
Torii, T., Yoshimura, T., Narumi, M., Hitoshi, S., Takaki, Y., Tsuji, S., Ikenaka, K., 2014. Glycoconj. J. 31, 671–683. https://doi.org/10.1007/s10719-014-9566-2.
Traving, C., Schauer, R., 1998. Cell. Mol. Life Sci. 54, 1330–1349. https://doi.org/10.1007/s000180050258.
Ullmann, V., Rädisch, M., Boos, I., Freund, J., Pöhner, C., Schwarzinger, S., Unverzagt, C., 2012. Angew. Chem. Int. Ed. 51, 11566–11570. https://doi.org/10.1002/anie.201204272.
Varki, A., 2008. Trends Mol. Med. 14, 351–360. https://doi.org/10.1016/j.molmed.2008.06.002.
Varki, A., 2007. Nature 446, 1023. https://doi.org/10.1038/nature05816.
Varki, A., Gagneux, P., 2012. Ann. N. Y. Acad. Sci. 1253, 16–36. https://doi.org/10.1111/j.1749-6632.2012.06517.x.
Von Itzstein, M., 2007. Nat. Rev. Drug Discov. 6, 967–974. https://doi.org/10.1038/nrd2400.
Von Itzstein, M., Wu, W.Y., Kok, G.B., Pegg, M.S., Dyason, J.C., Jin, B., Van Phan, T., Smythe, M.L., White, H.F., Oliver, S.W., Colman, P.M., Varghese, J.N., Ryan, D.M., Woods, J.M., Bethell, R.C., Hotham, V.J., Cameron, J.M., Penn, C.R., 1993. Nature 363, 418–423. https://doi.org/10.1038/363418a0.
Xiong, Y., Li, M., Lu, Q., Qing, G., Sun, T., 2017. Polymers (Basel), vol. 9. https://doi.org/10.3390/polym9070249.
Yang, G.Y., Li, C., Fischer, M., Cairo, C.W., Feng, Y., Withers, S.G., 2015. Angew. Chem. Int. Ed. 54, 5389–5393. https://doi.org/10.1002/anie.201411747.
Yonezawa, S., Sato, E., 1997. Pathol. Int. 47, 813–830. https://doi.org/10.1111/j.1440-1827.1997.tb03713.x.
Zhang, L., Wang, Y., Tian, Q., Liu, Y., Li, J., 2017. Biosens. Bioelectron. 89, 1013–1019. https://doi.org/10.1016/j.bios.2016.10.040.
Zhao, Q.L., Zhang, Z.L., Bao, L., Pang, D.W., 2008. Electrochem. Commun. 10, 181–185. https://doi.org/10.1016/j.elecom.2007.11.017.
Zhuravel, R., Amit, E., Elbaz, S., Rotem, D., Chen, Y.J., Friedler, A., Yitzchaik, S., Porath, D., 2016. Sci. Rep. 6, 6–11. https://doi.org/10.1038/srep36793.